SUPPORTING INFORMATION

Active Sites in Sn-Beta for Glucose Isomerization to Fructose and Epimerization to Mannose

Ricardo Bermejo-Deval[†], Marat Orazov[†], Rajamani Gounder** Son-Jong Hwang and Mark E. Davis*

Chemical Engineering, California Institute of Technology

Pasadena, CA 91125

*Corresponding author. E-mail: mdavis@cheme.caltech.edu

** Current address: School of Chemical Engineering, Purdue University, 480 Stadium Mall Drive, West Lafayette, IN 47907, USA

[†]R.B.D. and M.O. contributed equally to this work.

S.1. X-ray diffractograms of zeolite samples

Powder X-ray diffraction patterns of the samples in this study are shown in Figures S.1 and S.2.

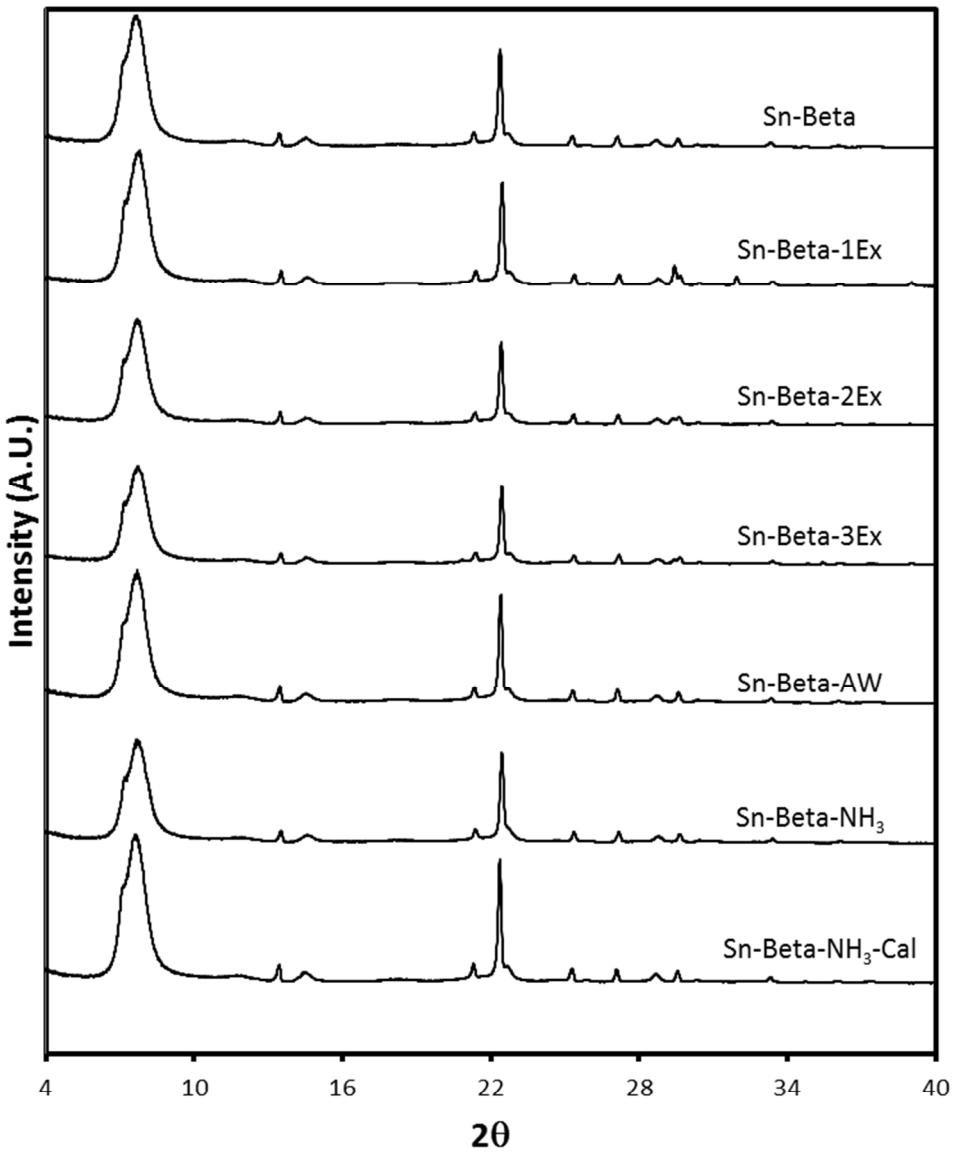

Figure S.1. Powder X-ray powder diffraction patterns of Sn-Beta, Sn-Beta-1Ex, Sn-Beta-2Ex, Sn-Beta-3Ex, Sn-Beta-AW, Sn-Beta-NH_3, and Sn-Beta-NH_3-Cal (top to bottom).

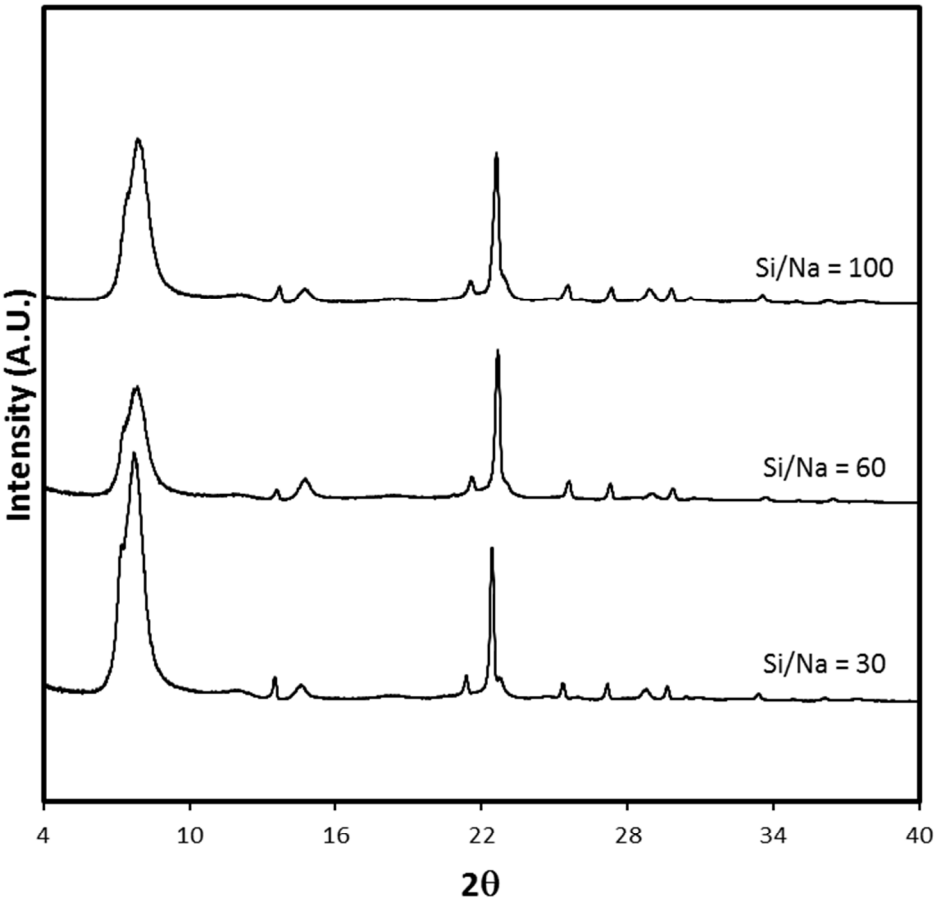

Figure S.2. Powder X-ray powder diffraction patterns of Sn-Beta with Si/Na synthesis gel composition of 100, 60, and 30.

S.2. SEM images of zeolite samples

SEM images of Sn-Beta, Sn-Beta-1Ex, Sn-Beta-3Ex, Sn-Beta-NH_3 and Na-Sn-Beta are shown at different magnifications in Figures S.3 and S.4.

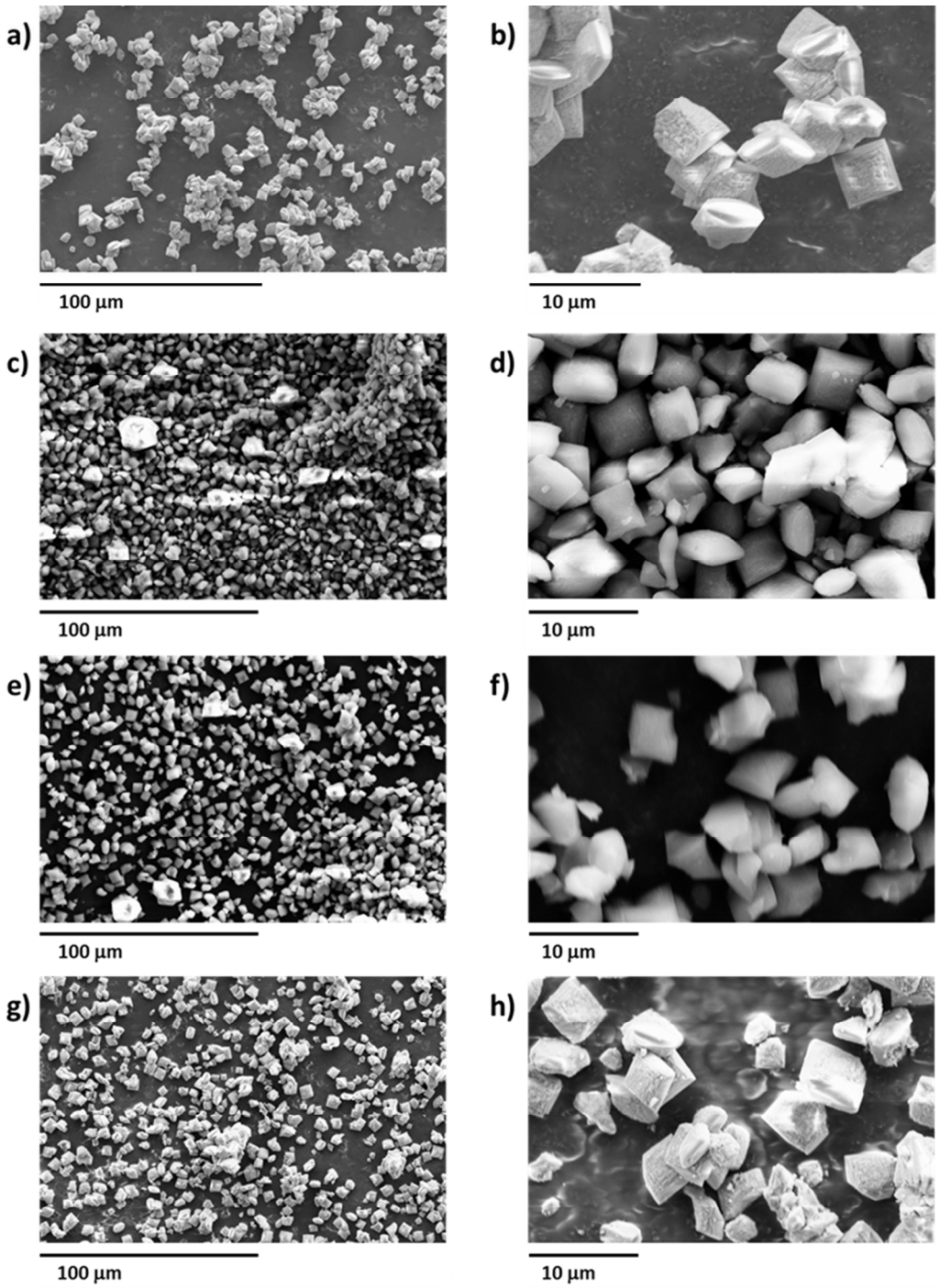

Figure S.3. SEM images of (a, b) Sn-Beta, (c, d) Sn-Beta-1Ex, (e, f) Sn-Beta-3Ex, and (g, h) Sn-Beta-NH_3.

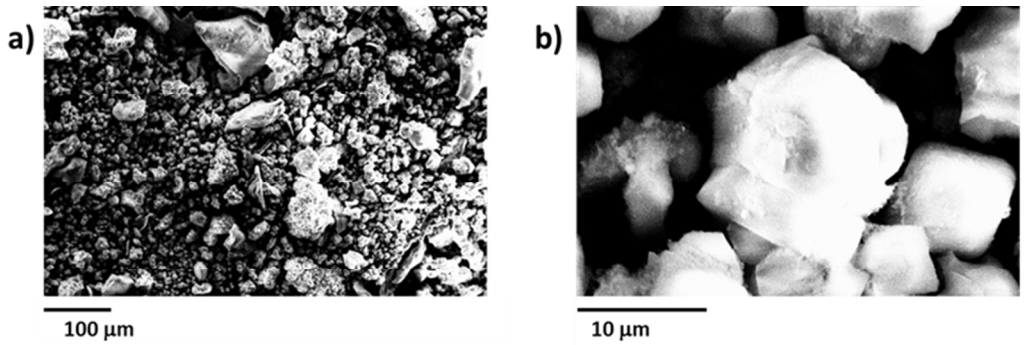

Figure S.4. SEM images of Na-Sn-Beta-30.

S.3. Ar adsorption isotherms of zeolite samples

Total micropore volume of each sample was determined from linear extrapolation of its Ar uptake in the mesopore regions (P/P_0 ~ 0.1-0.4) to zero relative pressure and from the liquid Ar molar density (0.035 mol cm^{-3}).

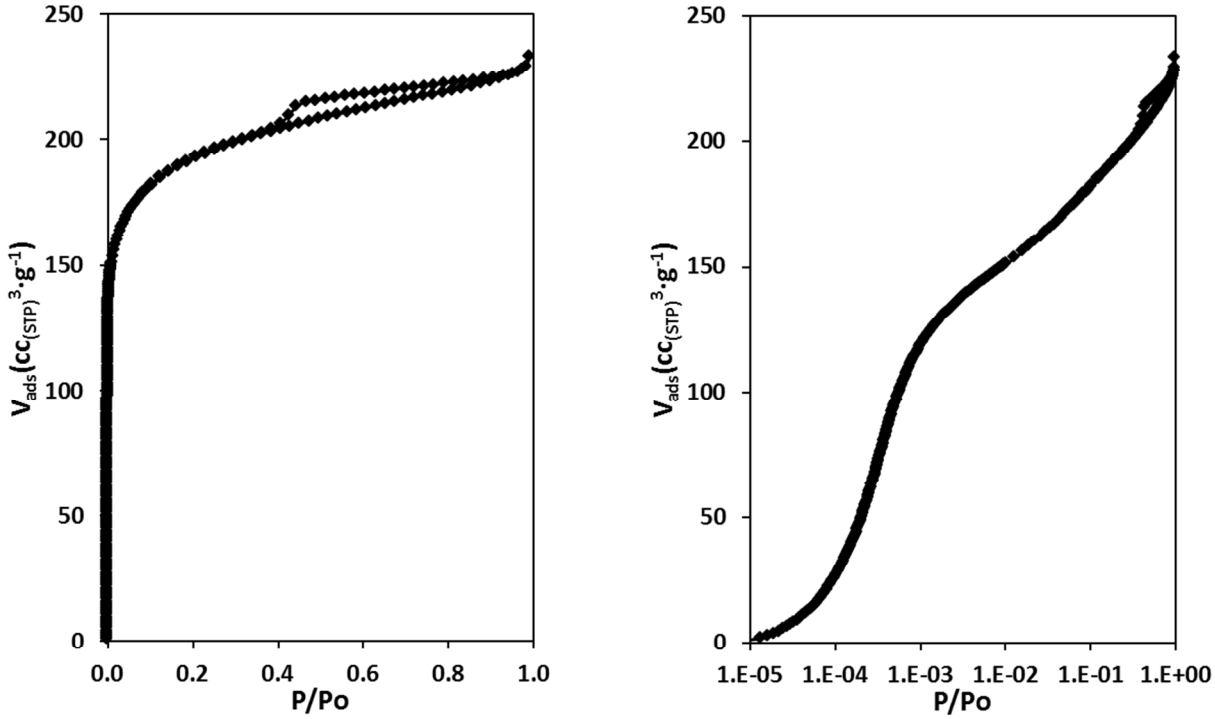

Figure S.5. Ar adsorption isotherm (87 K) for Sn-Beta.

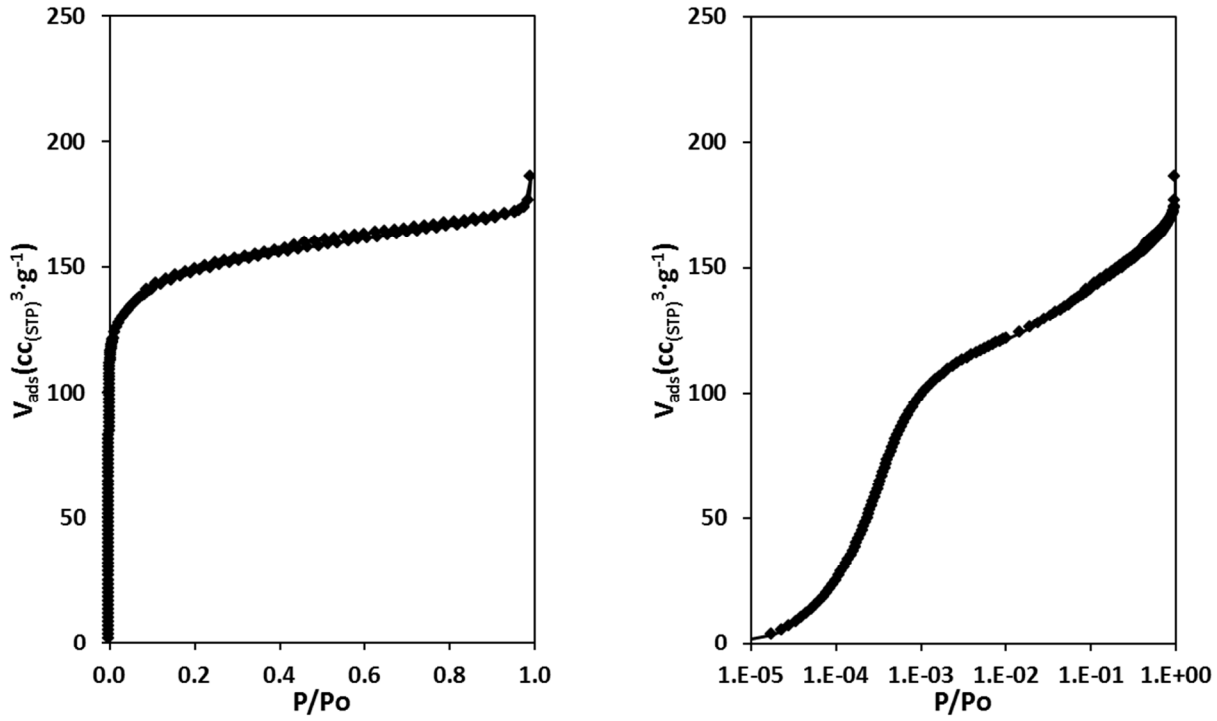

Figure S.6. Ar adsorption isotherm (87 K) for Sn-Beta-1Ex.

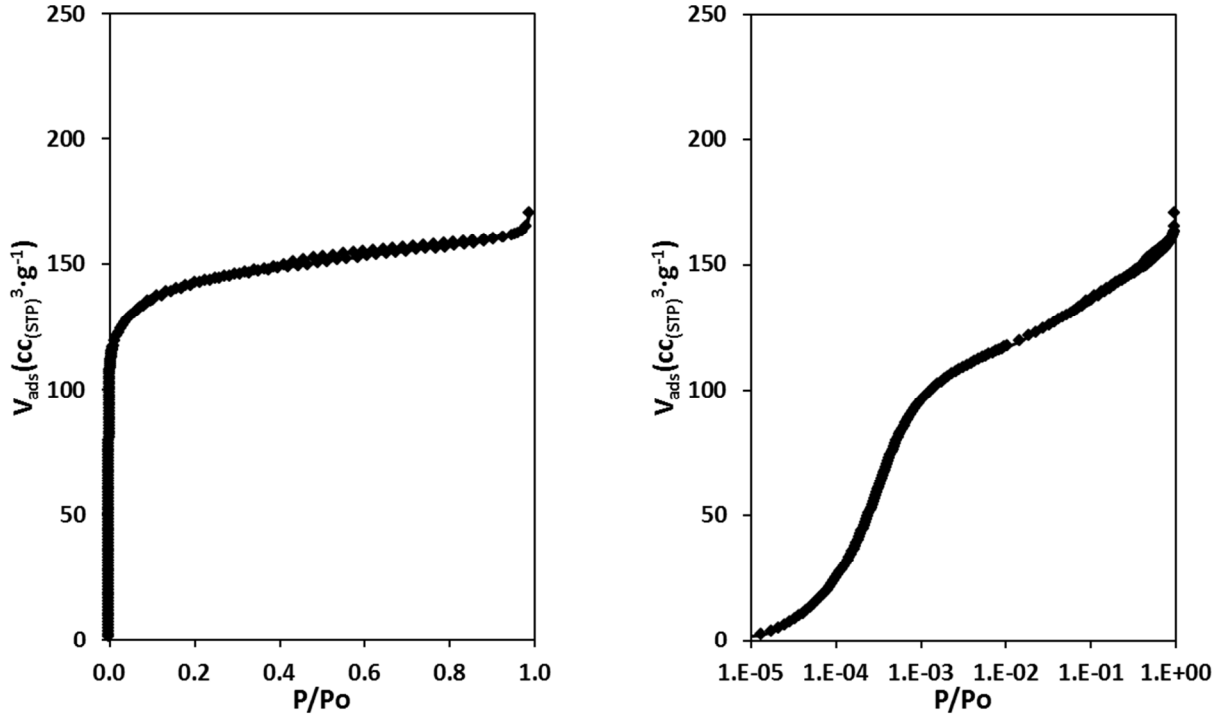

Figure S.7. Ar adsorption isotherm (87 K) for Sn-Beta-2Ex.

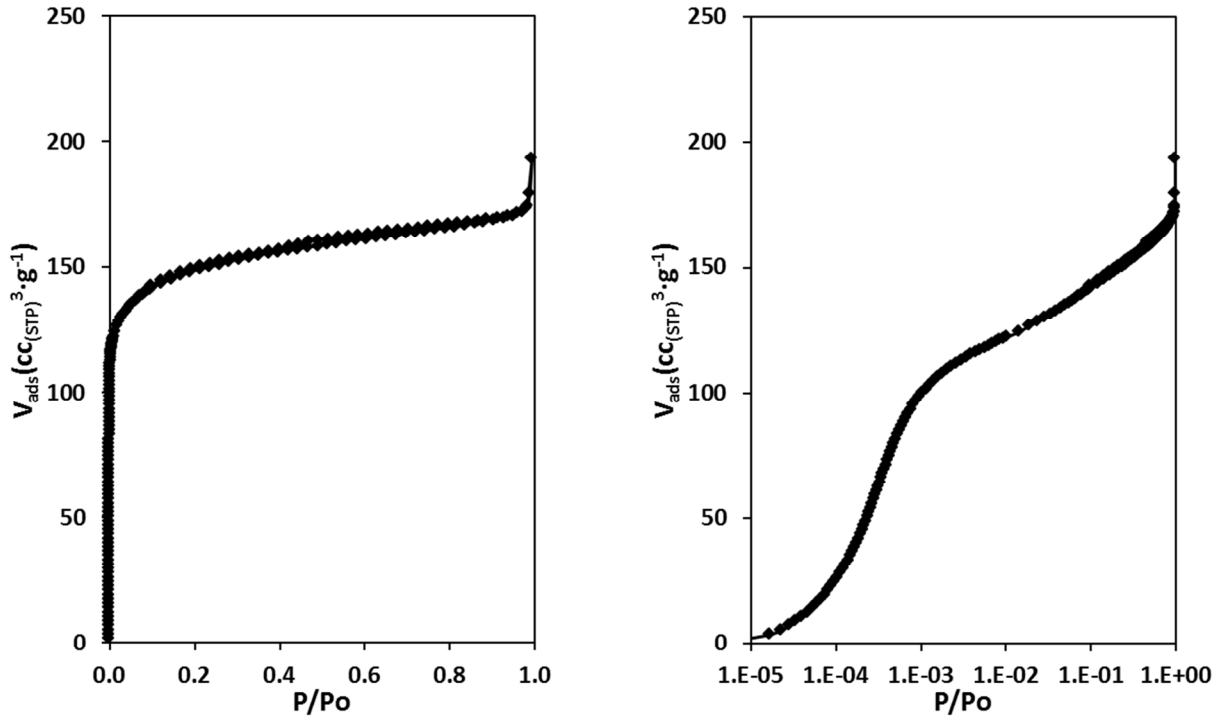

Figure S.8. Ar adsorption isotherm (87 K) for Sn-Beta-3Ex.

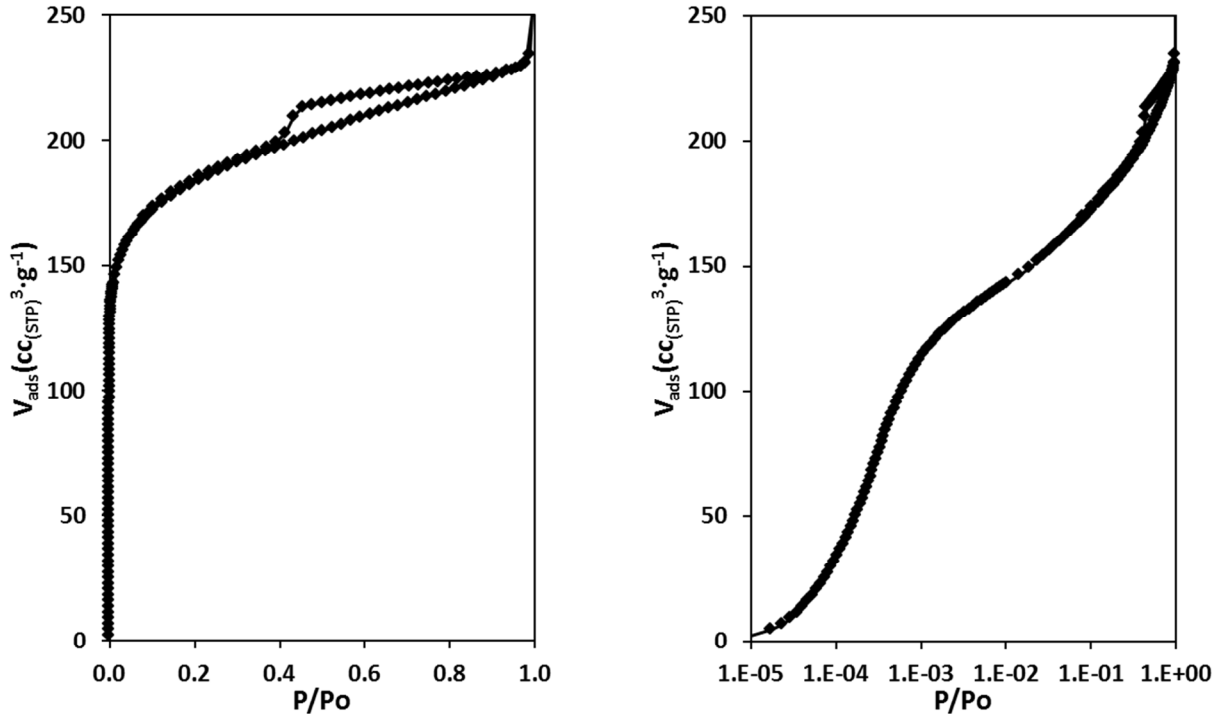

Figure S.9. Ar adsorption isotherm (87 K) for Sn-Beta-AW.

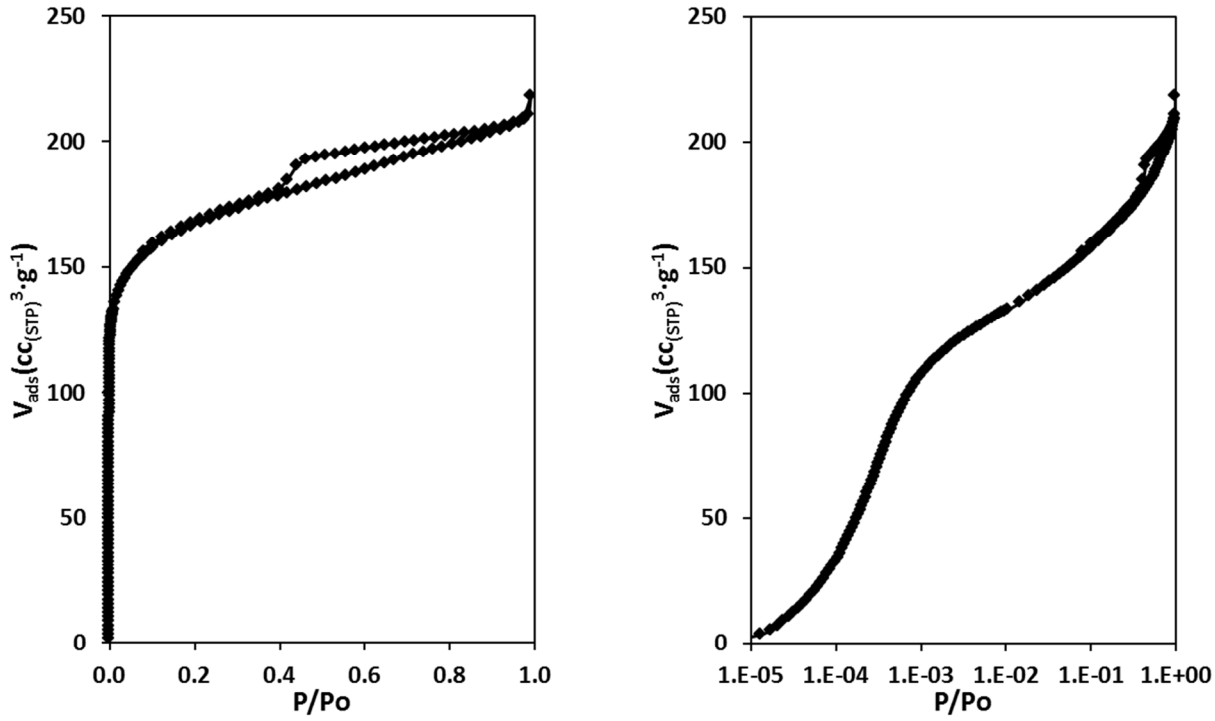

Figure S.10. Ar adsorption isotherm (87 K) for Sn-Beta-NH_3.

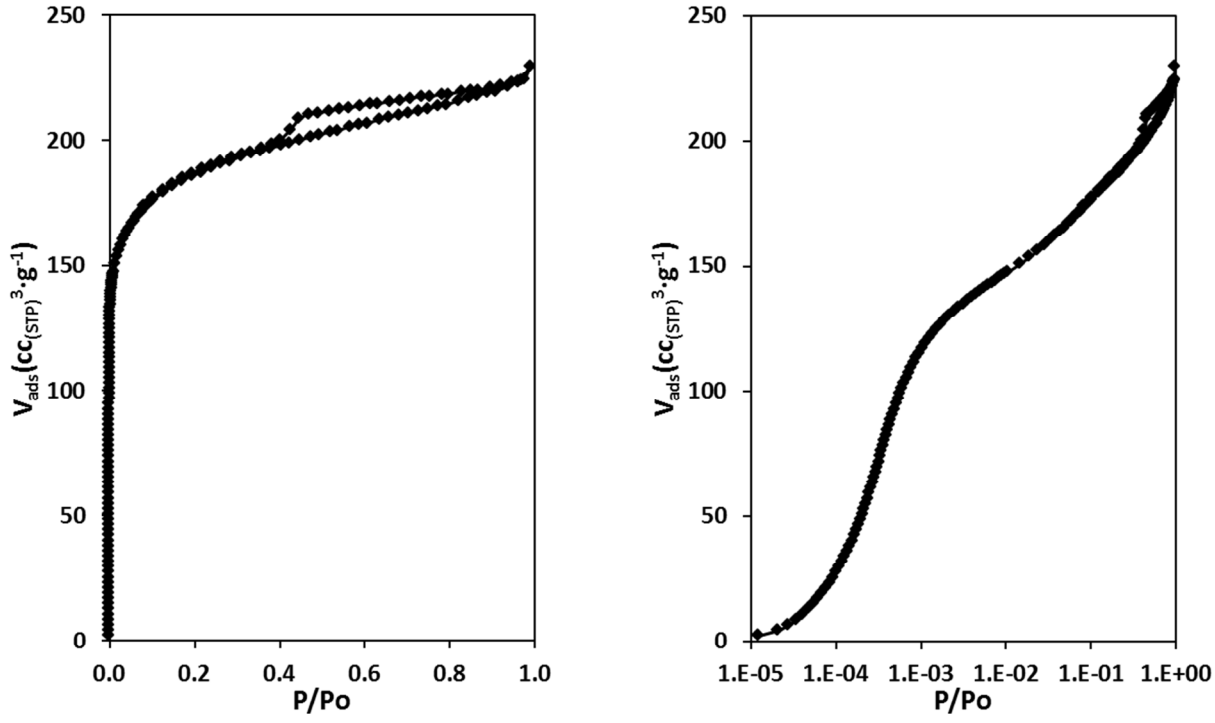

Figure S.11. Ar adsorption isotherm (87 K) for Sn-Beta-NH_3-Cal.

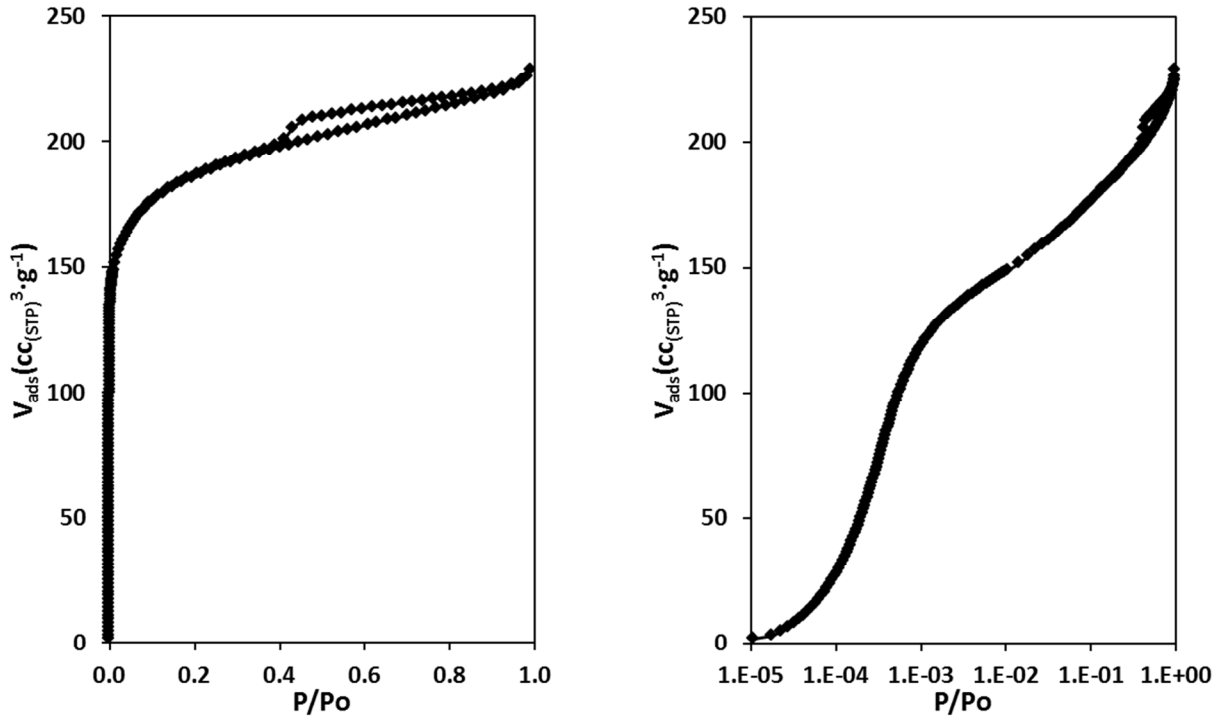

Figure S.12. Ar adsorption isotherm (87 K) for Na-Sn-Beta-100.

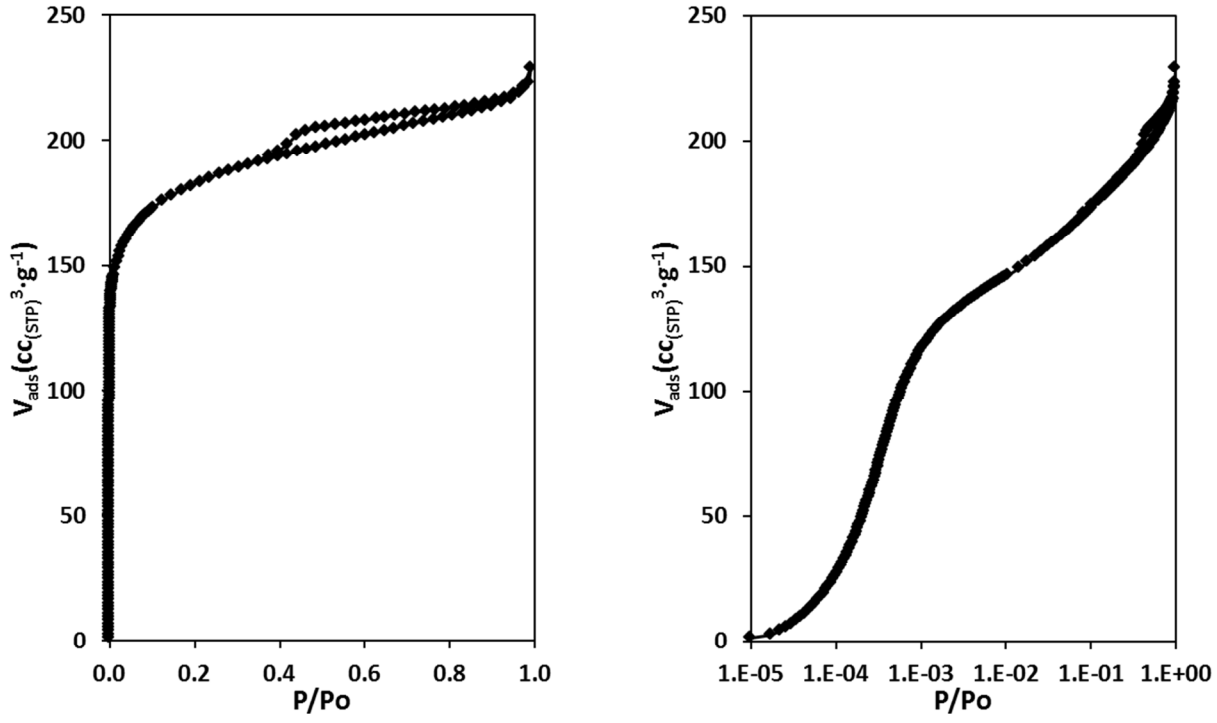

Figure S.13. Ar adsorption isotherm (87 K) for Na-Sn-Beta-60.

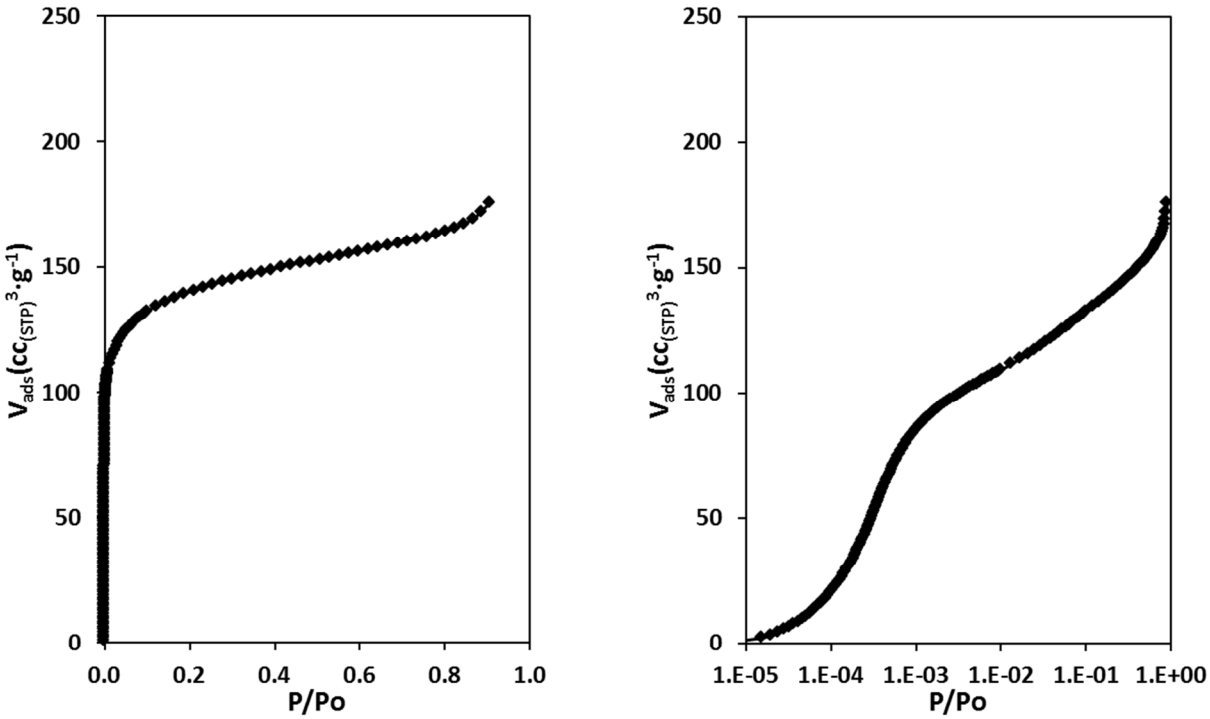

Figure S.14. Ar adsorption isotherm (87 K) for Na-Sn-Beta-30.

S.4. Infrared Spectroscopy

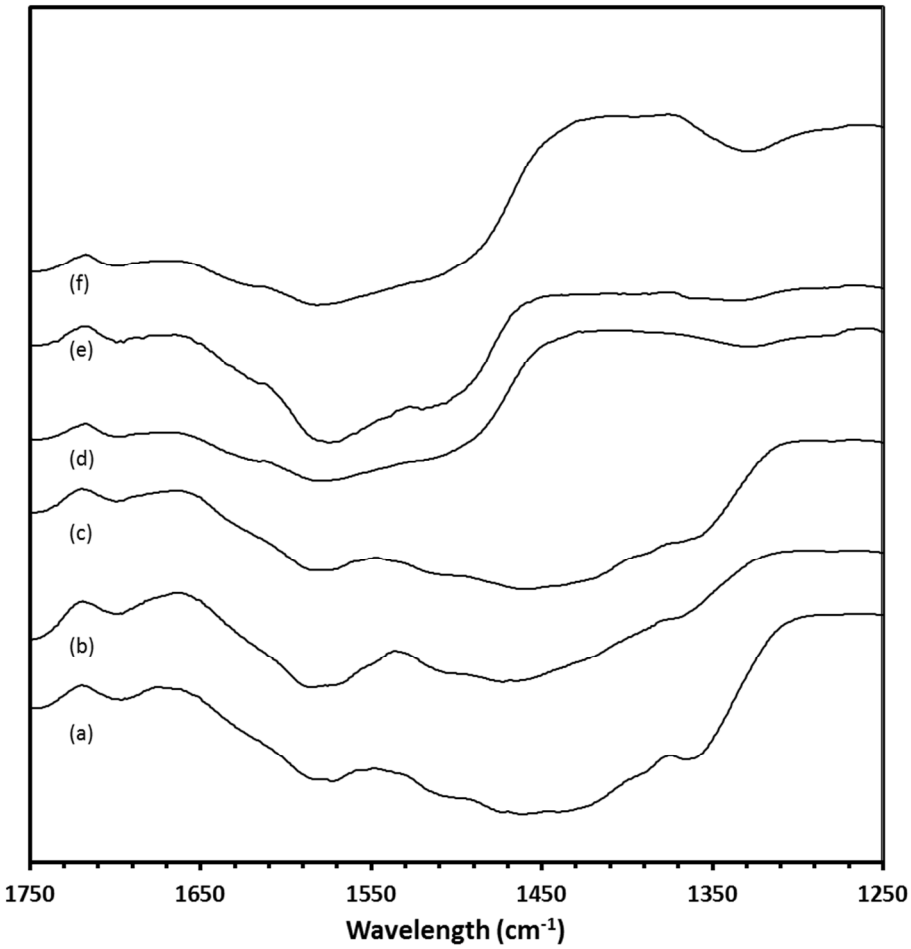

Figure S.15. IR spectra of (a) Sn-Beta, (b) Sn-Beta-AW, (c) Sn-Beta-NH_3-Cal, (d) Sn-Beta-1Ex, (e) Sn-Beta-2Ex, and (f) Sn-Beta-3Ex showing the presence or absence of a broad nitrate ion absorption band in the 1300 cm^{-1} -1500 cm^{-1} range.[1]

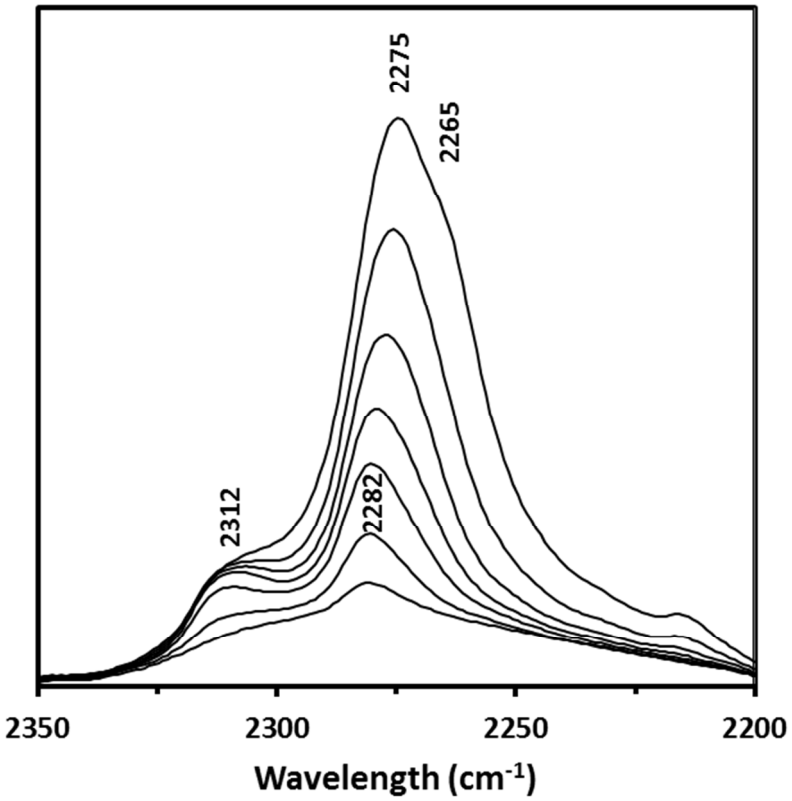

Figure S.16. Baseline corrected IR spectra with decreasing CD_3CN coverage on Sn-Beta-1Ex.

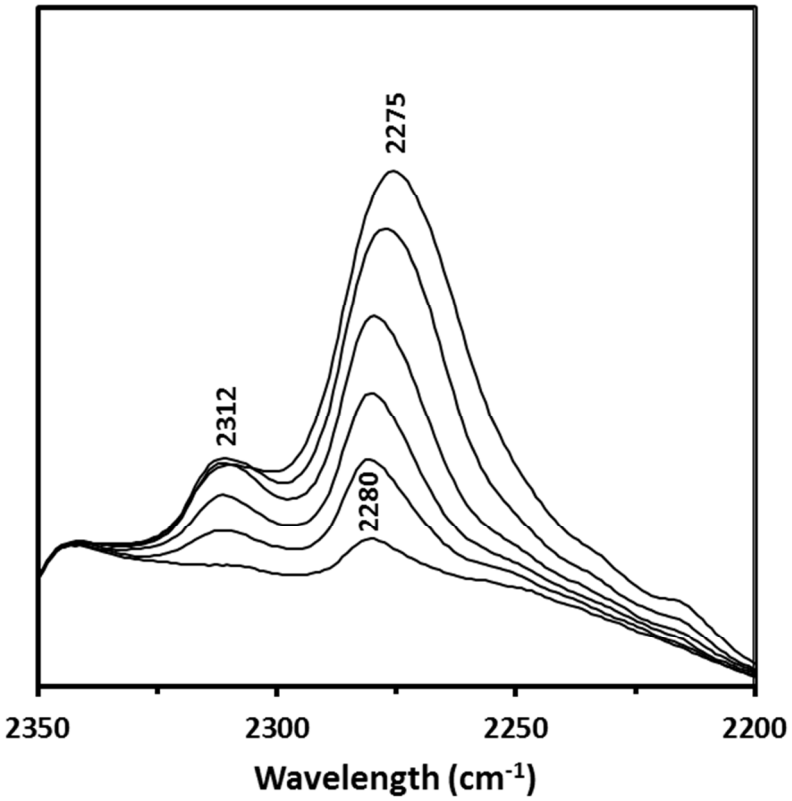

Figure S.17. Baseline corrected IR spectra with decreasing CD_3CN coverage on Sn-Beta-2Ex.

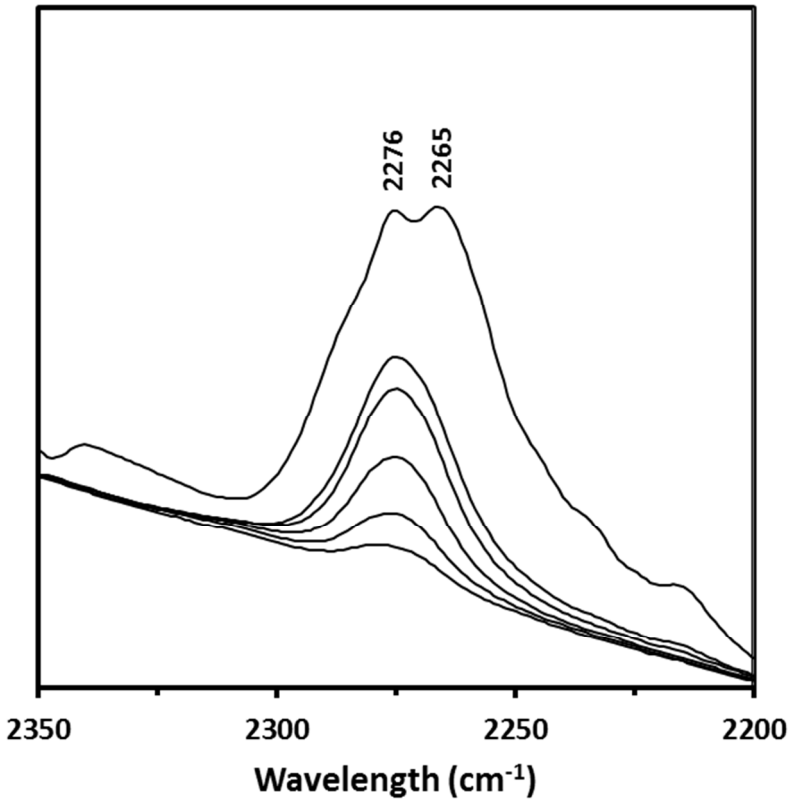

Figure S.18. Baseline corrected IR spectra with decreasing CD_3CN coverage on Si-Beta-3Ex.

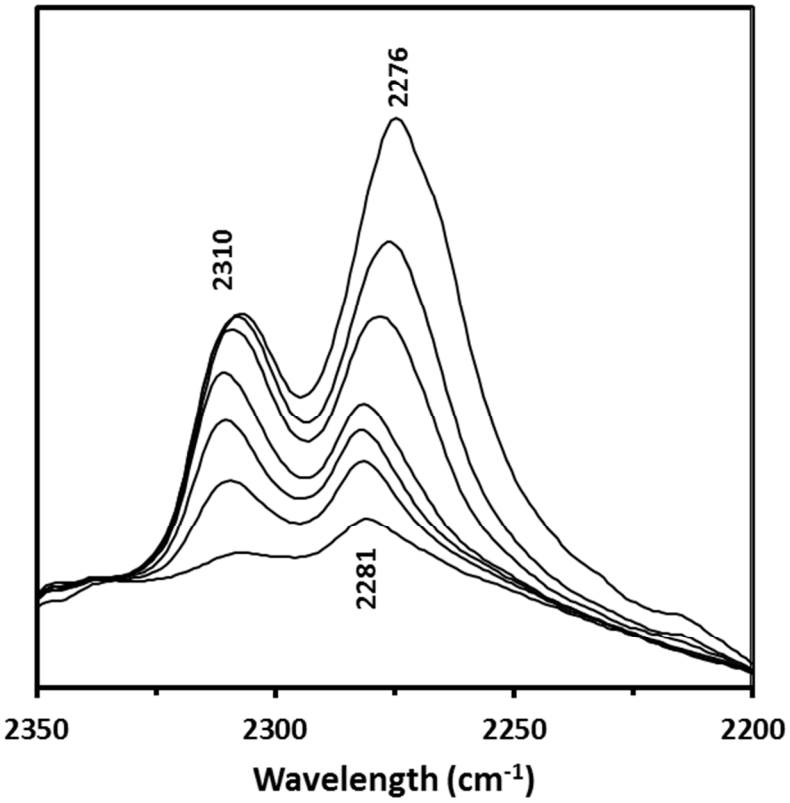

Figure S.19. Baseline corrected IR spectra with decreasing acetonitrile coverage on Na-Sn-Beta-30. This spectrum was collected after a 2h 773 K vacuum activation

S.5. Solid-State Magic Angle Spinning Nuclear Magnetic Resonance (SS MAS NMR)

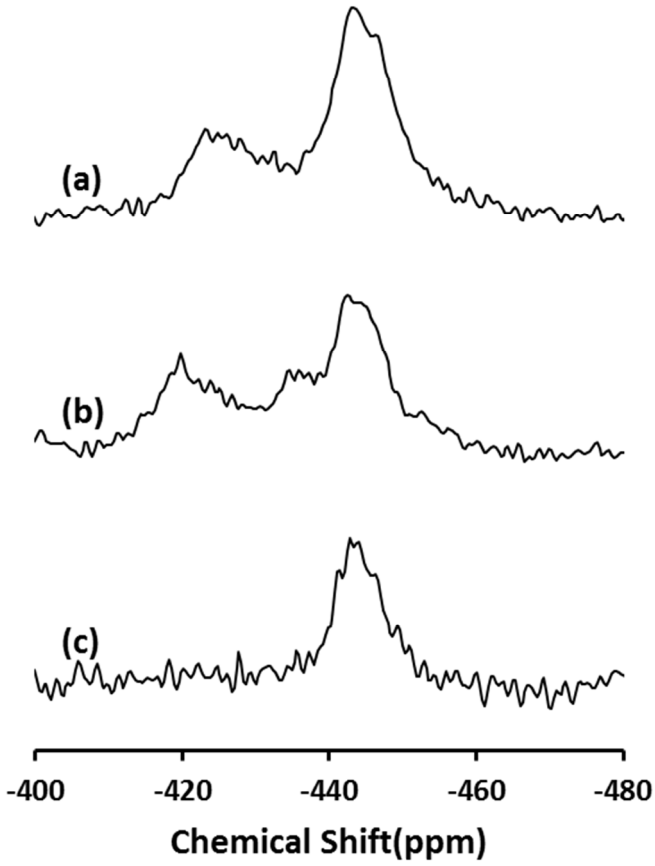

Figure S.20. Expanded chemical shift range in the -400 to -480 ppm region of ^{119}Sn MAS Solid State NMR spectra of ^{119}Sn-Beta after different treatments: (a) dehydration after calcination, (b) dehydration after three Na-exchanges and (c) dehydration after NH_3 adsorption.

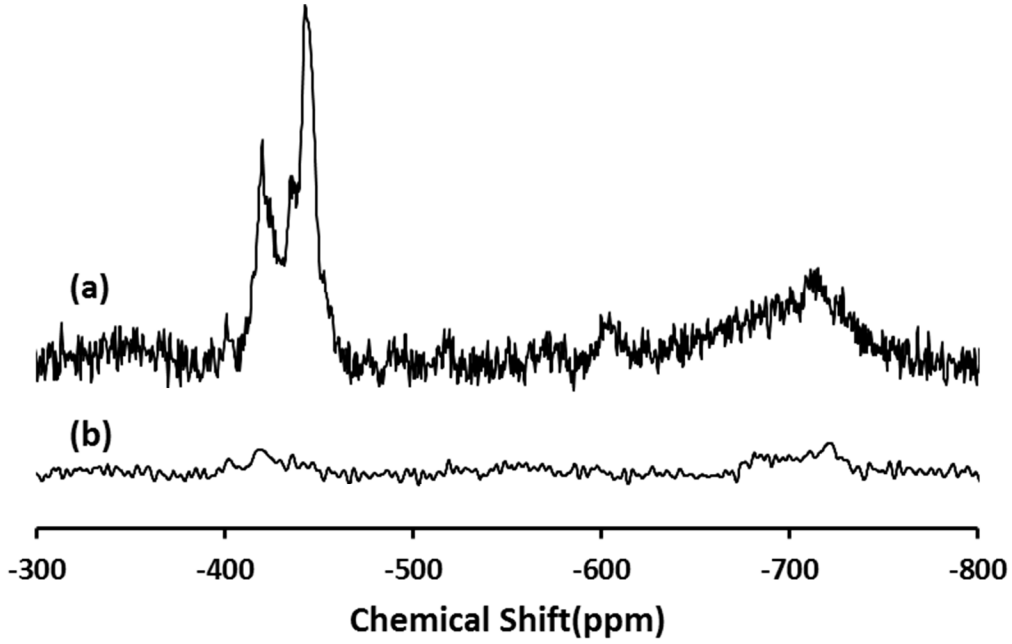

Figure S.21. ^{119}Sn NMR of three times Na-exchanged ^{119}Sn-Beta dehydrated at 397 K for 2h: (a) MAS spectrum and (b) CPMAS spectrum with 2ms contact time.

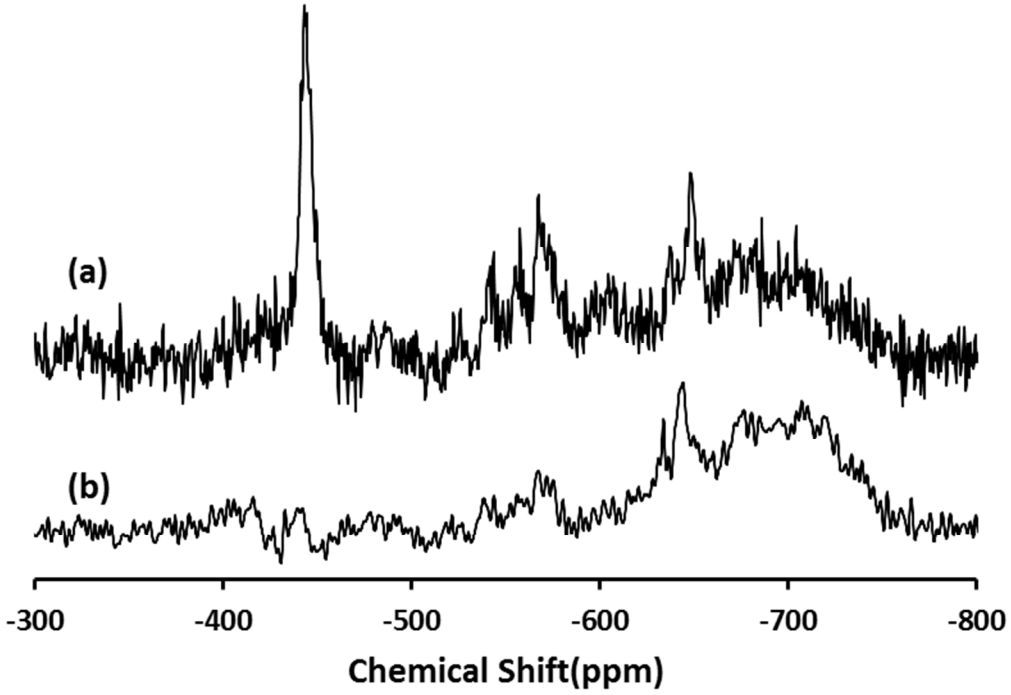

Figure S.22. ^{119}Sn NMR of NH_3-dosed ^{119}Sn-Beta dehydrated at 397 K for 2h: (a) MAS spectrum and (b) CPMAS spectrum with 2ms contact time.

S.6. Glucose conversion and fructose and mannose yields

Tables 2, 3, and 4 of the main text provide glucose conversion and fructose and mannose yields after 30 minutes of reaction. The following tables provide these data after 10 and 20 minutes of reaction.

Table S.1. Glucose conversion (X) and fructose and mannose yields (Y) in H_2O and CH_3OH solvents. Reaction conditions: 1% (w/w) glucose solutions, 1:100 metal:glucose ratio, 353 K, 10 and 20 min.

		10 minutes			*20 minutes*		
Catalyst	**Solvent**	$X_{Gluc.}(\%)$	$Y_{Fruc.}(\%)$	$Y_{Mann.}(\%)$	$X_{Gluc.}(\%)$	$Y_{Fruc.}(\%)$	$Y_{Mann.}(\%)$
Sn-Beta	H_2O	1.0	1.0	0.0	3.4	2.9	0.4
	CH_3OH	12.0	4.8	0.0	20.4	9.1	1.8
Sn-Beta-1Ex	H_2O	2.9	0.0	1.0	3.6	0.8	1.6
	CH_3OH	8.9	0.0	2.3	10.6	2.8	3.6
Sn-Beta-2Ex	H_2O	2.2	0.0	0.8	4.9	0.0	2.4
	CH_3OH	7.9	0.0	2.4	10.5	0.0	4.4
Sn-Beta-3Ex	H_2O	4.4	0.0	1.3	5.8	0.0	3.2
	CH_3OH	8.2	0.0	2.7	11.7	0.0	5.0
Sn-Beta-AW	H_2O	2.4	0.0	0.0	3.8	2.3	0.0
	CH_3OH	9.9	2.2	2.2	12.1	4.7	2.7
Na-Sn-Beta-100	H_2O	2.8	0.0	1.5	4.1	2.9	1.1
	CH_3OH	9.2	3.2	2.1	14.0	6.3	2.7
Na-Sn-Beta-60	H_2O	1.8	0.0	1.3	4.3	2.5	1.9
	CH_3OH	8.1	2.7	2.7	13.3	6.2	2.7
Na-Sn-Beta-30	H_2O	3.0	0.0	2.2	3.1	0.0	2.9
	CH_3OH	5.1	0.0	2.5	5.1	0.0	3.6
Sn-Beta-NH_3	H_2O	0.0	0.0	0.0	2.3	0.0	2.0
	CH_3OH	2.7	0.0	1.4	2.7	0.0	1.5
Sn-Beta-NH_3-Cal	H_2O	1.7	0.0	0.0	2.8	1.7	0.0
	CH_3OH	11.0	2.5	1.7	14.8	5.0	2.5

Table S.2. Glucose conversion (X) and fructose and mannose yields (Y) with 0.2g NaCl/g H_2O. Reaction conditions: 1% (w/w) glucose solutions, 1:100 metal:glucose ratio, 353 K, 10 and 20 min.

		10 minutes			*20 minutes*		
Catalyst	**Solvent**	$X_{Gluc.}(\%)$	$Y_{Fruc.}(\%)$	$Y_{Mann.}(\%)$	$X_{Gluc.}(\%)$	$Y_{Fruc.}(\%)$	$Y_{Mann.}(\%)$
Sn-Beta	H_2O-NaCl	5.1	1.9	2.1	9.6	3.4	3.2
Sn-Beta-1Ex	H_2O-NaCl	3.5	0.0	3.0	6.3	1.5	4.4
Sn-Beta-2Ex	H_2O-NaCl	4.0	0.0	3.0	5.8	1.4	5.0
Sn-Beta-3Ex	H_2O-NaCl	3.7	0.0	3.6	9.6	0.0	6.4

References

(1) Miller, F. A.; Wilkins, C. H. *Anal. Chem.* **1952**, *24*, 1253–1294.